1-1-2014

Analysis of fishscaling resistance of low carbon heavy plate steels

Aiwen Zhang
az483@uow.edu.au

Zhengyi Jiang
University of Wollongong, jiang@uow.edu.au

Dongbin Wei
University of Wollongong, dwei@uow.edu.au

Sihai Jiao
Baoshan Irong and Steel Co.

Chun Xu
Shanghai Institute of Technology

Analysis of fishscaling resistance of low carbon heavy plate steels

Abstract

The precipitates and hydrogen permeation behavior in three kinds of hot rolled low carbon heavy plate steels for enameling were analyzed; then, both sides of the steels were enameled. The experimental results show that a large amount of coarse Ti4C2S2 and fine Ti(C, N) particles exist in the optimized Ti-bearing steel, quite a lot of fine Ti(C, N) particles exist in the optimized carbon steel, but only a little bit fine Ti(C, N) particles exist in the carbon steel. The fishscaling resistance of the steels can be correlated to the effective hydrogen diffusion coefficient, and a model of correlation between the effective hydrogen diffusion coefficient and the volume fraction of the precipitates was established and verified. The effective hydrogen diffusion coefficient should be lower than 3. 96 x 10 6 cm2/s to avoid fishscaling in heavy plate steels.

Keywords

fishscaling, resistance, plate, low, heavy, carbon, analysis, steels

Disciplines

Engineering | Science and Technology Studies

Publication Details

Zhang, A., Jiang, Z., Wei, D., Jiao, S. & Xu, C. (2014). Analysis of fishscaling resistance of low carbon heavy plate steels. Journal of Iron and Steel Research International, 21 (4), 469-475.

Analysis of Fishscaling Resistance of Low Carbon Heavy Plate Steels

Ai-wen ZHANG[1], Zheng-yi JIANG[1], Dong-bin WEI[1],
Si-hai JIAO[2], Chun XU[3]

(1. Faculty of Engineering, University of Wollongong, Wollongong 2522, NSW, Australia; 2. Research Institute, Baoshan Iron and Steel Co., Ltd., Shanghai 201900, China; 3. Department of Material Science and Engineering, Shanghai Institute of Technology, Shanghai 201418, China)

Abstract: The precipitates and hydrogen permeation behavior in three kinds of hot rolled low carbon heavy plate steels for enameling were analyzed, then both sides of the steels were enameled. The experimental results show that a large amount of coarse $Ti_4C_2S_2$ and fine Ti(C, N) particles exist in the optimized Ti-bearing steel, quite a lot of fine Ti(C, N) particles exist in the optimized carbon steel, but only a little bit fine Ti(C, N) particles exist in the carbon steel. The fishscaling resistance of the steels can be correlated to the effective hydrogen diffusion coefficient, and a model of correlation between the effective hydrogen diffusion coefficient and the volume fraction of the precipitates was established and verified. The effective hydrogen diffusion coefficient should be lower than 3.96×10^{-6} cm^2/s to avoid fishscaling in heavy plate steels.

Key words: fishscaling resistance; hydrogen permeation; precipitate; enameling

Fishscale is one of the worst defects in the production of enameled steel products[1]. It is caused by an excess of hydrogen which dissolves into the steel during the enameling process, especially during the enamel firing at the temperature of 800－850 ℃. Since its solubility steeply decreases during subsequent cooling, hydrogen moves toward the steel-enamel interface in quantities that can cause fishscaling even after a lapse of time. When the steel is enameled, whether the fishscaling happens or not, it depends on the chemical compositions, the trapping sites, such as microvoids, dislocations and precipitates, and eventually the hydrogen permeation behavior in the steel. The hydrogen diffusivity in steel has an obvious effect on the fishscaling resistance[2]. The lower the hydrogen permeability, the lower the fishscaling susceptibility. It is reported that the hydrogen diffusion coefficient should be lower than 2.0×10^{-6} cm^2/s to avoid fishscaling when the sheet steels were enameled[3], the trapping sites significantly influence the hydrogen solubility and diffusivity[4, 5].

The trapping sites can be classified into reversible and irreversible types according to the binding energy (E_b in eV) with the hydrogen atoms[6]. Normally, dislocations and grain boundaries, which have a lower E_b about 0.25－0.27 eV, are reversible sites; inclusions, precipitates and microvoids, on the contrary, with a higher E_b about 0.80－0.98 eV, are irreversible sites. In the hot rolled steels for enameling, the precipitates or inclusions are main irreversible sites for hydrogen. The effects of these particles on the fishscaling resistance have been studied by many researchers[7-12]. Valentini et al.[13, 14] established a model to quantitatively assess the fishscaling susceptibility using the free hydrogen parameter. However, most of the researches on fishscaling resistance have been done on hot or cold rolled sheet steels, fewer on hot rolled heavy plate steels. Nowadays, there are increasingly demands for heavy plate enameling steels, for example, steels used for chemical reaction vessels, silos. These steels, which are normally in thickness of about 12－25 mm, will be enameled one side or both sides, then fishscaling may occur and show a different susceptibility from the sheet steels. So, this paper will focus on

the fishscaling resistance of hot rolled low carbon heavy plate steels for enameling, the precipitates, hydrogen permeation behavior and enameling process were all studied.

1 Experimental

A carbon steel (named CB), an optimized carbon steel (named OCB) and an optimized Ti-bearing steel (named OTB) were designed in laboratory, and then vacuum-melting, ingot casting, forging and slab hot rolling process were carried out. The slabs were reheated at 1200 ℃, and then hot rolled to heavy plates with a thickness of 16 mm at the finishing temperature of 880 ℃, and then air cooled to the room temperature. The yield strengths of the three steels are between 265 to 290 MPa. The CB steel does not contain vanadium and just has a little bit titanium, vanadium was added in the OCB steel but the carbon content was decreased, and the OTB steel has a higher content of titanium but a lower carbon content than that of the OCB steel. The variation of such elements content is to maintain the yield strength and to modify the fishscaling resistance of the steels. The chemical compositions for the three developed steels are shown in Table 1.

Table 1 Chemical compositions of the developed steels mass%

Steel	C	Mn	S	Al	Ti	V	N
CB	0.144	0.85	0.004	0.046	0.015		0.0048
OCB	0.092	0.84	0.004	0.041	0.016	0.047	0.0056
OTB	0.069	0.70	0.010	0.040	0.050	0.052	0.0087

The precipitates in the steels were extracted on carbon replicas and examined by an FEI Tecnai G^2 high resolution transmission electron microscope (HRTEM) equipped with an energy dispersive spectrometer (EDS). Selected area electron diffraction (SAD) patterns combined with EDS analysis were used to identify the precipitates. The quantitative analysis of the precipitates was carried out using the ordinary quantitative metallographic methods, that is to measure the average diameter d and the number of the particles per unit area N_s from the electron micrograph. The relative error of the particle diameter is less than 8% under 95% confidence level. The particle volume fraction V_f and the number of particles per unit volume N_v can be calculated by the Fullman formula

$$V_f=\pi/6\cdot N_s\cdot d^2 \quad (1)$$

$$N_v=N_s/d \quad (2)$$

Hydrogen permeation was measured using an electrochemical method developed by Devanathan and Stachurki[6]. Square samples of 1.2 mm×50 mm×50 mm were cut from different locations in the thickness of the heavy plates, ground to 1 mm in thickness and then electrolytic polished. Put the samples into 20% HCl electrolyte and made a cathodic polarization treatment for 10 to 20 s with current density of 21.5 mA/cm^2. After immersed and washed by anhydrous ethanol and toluene, the samples were then immediately one-side electroplated with 0.05 to 0.10 μm Pd layer. The prepared specimen was installed in a CS-330 electrochemistry workstation, European standard (NF EN ISO 17081) was adopted for measurement. The bare face of the specimen is for charging the hydrogen, and the Pd electroplated face is diffusion face. Both cathodic and anodic solutions were 0.1 mol/L NaOH, which were deaerated with N_2 to avoid the cathodic reaction due to O_2. The charging current density was maintained at 1.8 mA/cm^2, and then began to record the anode current with different times on

the diffusion face, until the anode current reaches a steady state (the maximum value).

The effective diffusion coefficient of hydrogen D_{eff} can be calculated from the hydrogen permeation curves by the time lag method[4, 6]

$$D_{\text{eff}} = L^2 / 6t_{\text{T}} \quad (3)$$

where L denotes the specimen thickness and t_T denotes the lag time. The lag time can be obtained by spotting the time at which the permeation rate is 0.63 times the steady-state value, namely normalized output flux J_t/J_∞ =0.63[6]. Hydrogen trap parameter α is also calculated using the following equation for assessing the fishscaling resistance of steel

$$\alpha = -1 + t_{\text{T}} / t_{\text{L}} \quad (4)$$

where

$$t_{\text{L}}=L^2/6D_L$$

$$D_{\text{L}}=D_0\exp(-Q/RT)$$

t_L is the lag time of hydrogen in metal lattice without trapping sites; D_L is the hydrogen diffusion coefficient in metal lattice without trapping sites. D_0 and Q are 0.78×10^{-3} cm^2/s and 7950 J/mol, respectively [5]. $D_L=2.9843\times10^{-5}cm^2/s$ when temperature is 293 K.

The both sides of the steels were enameled, and the enamel frit consists of more than 60% of SiO_2 and the other oxides. The ground coat and six overglazes were sprayed and fired in turn. The firing temperatures are between 870 and 920 ℃. The thickness of the enamel layer is about 1 mm. The enameled heavy plates were observed by the naked eyes for fishscales. The small cross-sectional samples cut from the enameled heavy plates were mounted, ground and polished, and then the samples were examined by a Leica DMR-HC optical microscope (OM) for traces of fishscaling.

2 Results and Discussion

2.1 Precipitates analysis

Fig. 1 shows the precipitates shape, size and distribution on carbon replicas of the developed steels. It can be seen that the precipitates exhibit the different quantity, grade and distribution in each steel. Two kinds of precipitates of different shape and size are observed, one is the larger round or elliptic particles with size about 50 －250 nm, it mainly exists in the OTB sample; the other is the smaller square or rectangular particles with size about 10－40 nm, it mainly exists in the OCB and CB samples, but the quantity of the smaller particles in the OCB sample is higher than that in the CB sample.

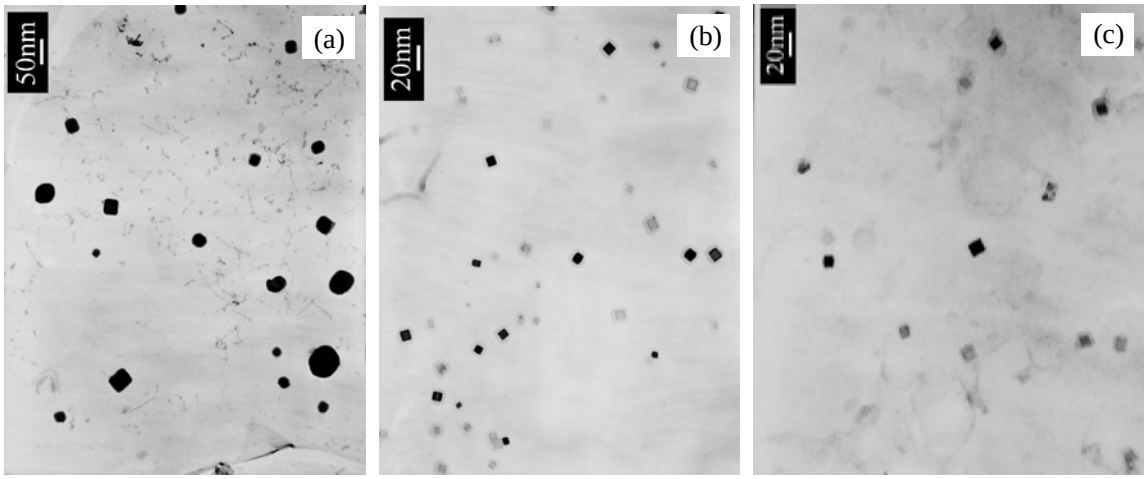

(a) OTB; (b) OCB; (c) CB.

Fig. 1 Quantity, shape and distribution of precipitates on carbon replicas

The morphology, composition and structure of these particles were analyzed by a TEM combined with an EDS and an SAD. After a large number of EDS spectrum analyses, the results show that the large particles in the OTB sample are hexagonal structure $Ti_4C_2S_2$ and face-centered cubic (FCC) Ti(C, N), as well as a small amount of MnS. The size and morphology of MnS particle are similar to $Ti_4C_2S_2$, but the EDS spectrum ingredients can distinguish it. If the Ti and S atoms ratio is close to 2, it can be basically identified as $Ti_4C_2S_2$; if the Mn and S atoms ratio is close to 1, and then it may be identified as MnS. The fine particle in the OTB sample has a square or rectangular shape, the EDS analysis shows that the fine particle is FCC Ti(C, N), because C and N cannot be distinguished by EDS on a carbon replica. Fig. 2 shows the morphology and EDS spectrum analysis of $Ti_4C_2S_2$.

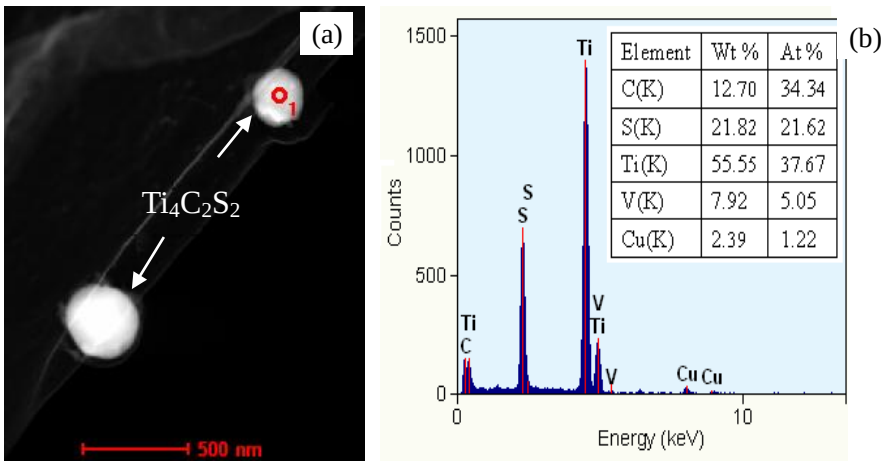

(a) $Ti_4C_2S_2$ particles; (b) EDS spectrum of $Ti_4C_2S_2$ marked in (a).

Fig. 2 TEM analysis of particles in OTB sample

The shape of the particles in the CB sample is mainly rectangular or square, and the size of the most particles is normally less than 50 nm. Fig. 3 shows the morphology, SAD pattern and EDS spectrum analysis of a rectangular or square particle. In this study, it can be found that the particles almost have the same FCC structure and similar compositions, which are identified as Ti(C, N). The shape and size of the particles in the OCB sample are similar to the CB sample. However, the quantity of the particles in the OCB sample is more than that in the CB

sample. Most of the particles in the OCB sample are also FCC Ti(C, N).

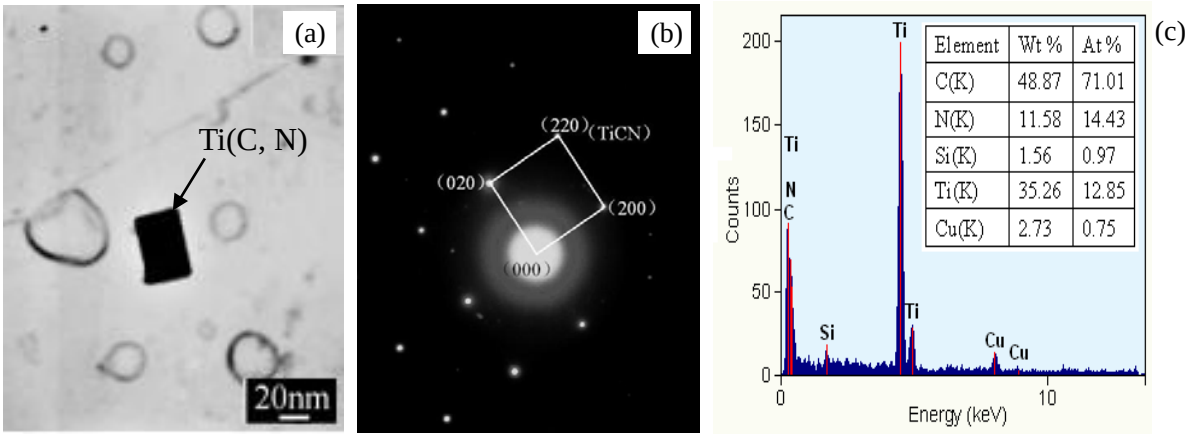

(a) Morphology of particles; (b) SAD pattern of particle marked in (a); (c) EDS spectrum of particle marked in (a).

Fig. 3 TEM analysis of particles in CB sample

Actually there are also other phases exist in the OCB and OTB samples due to the vanadium addition. V(C, N) particles have been observed in such two steel samples. The V(C, N) particles can precipitate during the finish rolling temperature (880 ℃) and also the air cooling process[15].

The quantitative analyses of these precipitates are listed in Table 2. The d and N_s were measured from the electron micrographs, and then N_v and V_f can be calculated by Eqs. (1) and (2). It can be seen that the numbers per unit volume of Ti(C, N) in the OTB sample is much higher than those in the OCB and CB samples, but the mean size of the Ti(C, N) in the OTB sample is about half of those in the OCB and CB samples. The volume fraction of Ti(C, N) in the OTB sample is less than those in the OCB and CB samples. $Ti_4C_2S_2$ in the OTB sample consists of the most volume fraction, so the total volume fraction of the particles in the OTB sample is the highest at 0.152%, which is about double of that in the OCB sample and four times of that in the CB sample. The quantitative analysis result is in good agreement with the chemical compositions, because the OTB steel has the highest Ti, V , N and S contents.

Table 2 Quantitative analysis of precipitates in the three steels for enameling

Sample	Precipitate	d/nm	N_v/(10^{20} particles·m^{-3})	V_f/%
OTB	Ti(C, N), V(C, N)	11.0	4.569	0.032
	$Ti_4C_2S_2$	71.3	0.063	0.120
OCB	Ti(C, N), V(C, N)	21.7	1.388	0.074
CB	Ti(C, N)	25.3	0.474	0.040

2.2 Hydrogen permeation behavior

The hydrogen permeation curves at different temperatures are shown in Figs. 4(a), 4(b) and 4(c). It can be seen that the hydrogen diffusion is accelerated with an increase of temperature. The hydrogen diffusion in the OTB sample is slower than those in the OCB and CB samples when the measured temperature is the same. From

the curves, the lag times of hydrogen permeations at different temperatures can be obtained, and then D_{eff} and α can be calculated by Eqs. (3) and (4). Fig. 4(d) shows the effective diffusion coefficient as a function of the reciprocal temperature. The activation energies Q for hydrogen diffusion in the three steel samples are calculated according to the slope of the line. The t_T, D_{eff}, Q and α are listed in Table 3.

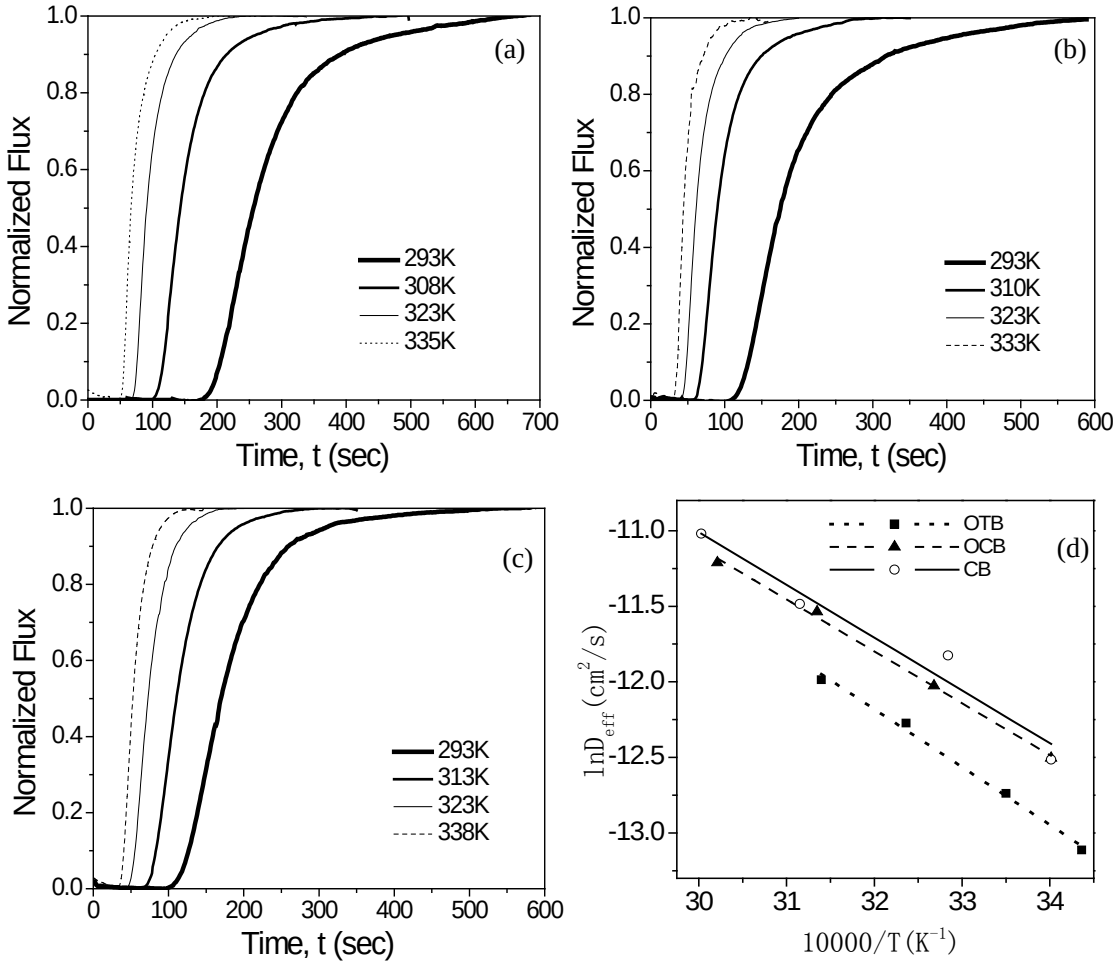

(a) Normalized hydrogen output flux of the OTB samples; (b) Normalized hydrogen output flux of the OCB samples; (c) Normalized hydrogen output flux of the CB samples; (d) Effective diffusion coefficient of the three steels.

Fig. 4 Normalized hydrogen output flux and effective diffusion coefficient of the three steels

Table 3 Hydrogen permeation results for the three samples at 293 K

Parameter	OTB	OCB	CB
L/cm	0.0726	0.0690	0.0733
t_T/s	282	200	206
D_{eff}/(cm^2·s^{-1})	3.11×10^{-6}	3.96×10^{-6}	4.35×10^{-6}
Q/(kJ·mol^{-1})	29.01	28.10	28.09
α	8.58	6.53	5.86

The activation energies for hydrogen diffusion are 29.01, 28.10 and 28.09 kJ/mol in the OTB, OCB and CB samples, respectively. These values are larger than those of dislocations (25.6 kJ/mol) and roughly equal to

microvoids (29.1 kJ/mol)[16]. This means that the precipitates existed in the samples can act as the irreversible trapping sites for hydrogen atoms, which have similar function as the microvoids. The number of irreversible trapping sites can be correlated with the volume fraction of precipitates[7]. As shown in Table 2, the total volume fraction of precipitates in the OTB steel is larger than those in the OCB and CB steels. So, the OTB steel has much more irreversible trapping sites than the OCB and CB steels. Irreversible trapping of hydrogen atom leads to a large decrease in hydrogen diffusivity[17]. Therefore, it is reasonable that the hydrogen diffusivity in the OTB sample is much lower, which is in good agreement with the hydrogen permeation results listed in Table 3.

2.3 Modeling of correlation between effective hydrogen diffusion coefficient and volume fraction of irreversible trapping sites in enameling steel

From Eqs. (3) and (4), the relationship between D_{eff} and α can be expressed as Eq. (5)

$$D_{\text{eff}} = D_{\text{L}} /(1+\alpha) \tag{5}$$

D_{eff} has a reciprocal relationship with $1+\alpha$. D_{L} will be a constant if the temperature is fixed. If there are no trapping sites in metal, then t_{T} is equal to t_{L}, and α is equal to 0, then D_{eff} is equal to D_{L}.

Plotting α at temperature of 293 K *vs.* V_{f} of the precipitates (irreversible sites) in the three steels and fitting the symbol with linear regression, the graph was shown in Fig. 5. It can be seen that α is proportional to V_{f}, and r^2 of the linear regression is equal to 0.99211, that means the accuracy of the linear relationship between α and V_{f} is very high. The function between α and V_{f} can be expressed as Eq. (6) according to the regression

$$\alpha = 24.728V_{\text{f}} + 4.801 \tag{6}$$

Substituting α in the Eq. (5) by α in the Eq. (6), and applying the data of D_{L} (2.9843×10^{-5}cm^2/s) at 293 K, then the relationship between D_{eff} and V_{f} is

$$D_{\text{eff}} = 1.2069\times10^{-6} /(0.2346+V_{\text{f}}) \tag{7}$$

Using the V_f data listed in Table 2 and the L and t_{T} data listed in Table 3, then the D_{eff} can be calculated by Eqs. (3) and (7), respectively. Table 4 shows the effective hydrogen diffusion coefficients calculated by Eq. (7). From Tables 3 and 4, it can be seen that the D_{eff} calculated by Eq. (7) is very close to the D_{eff} calculated by Eq. (3). This result testify the regressed relationship between α and V_f is accurate.

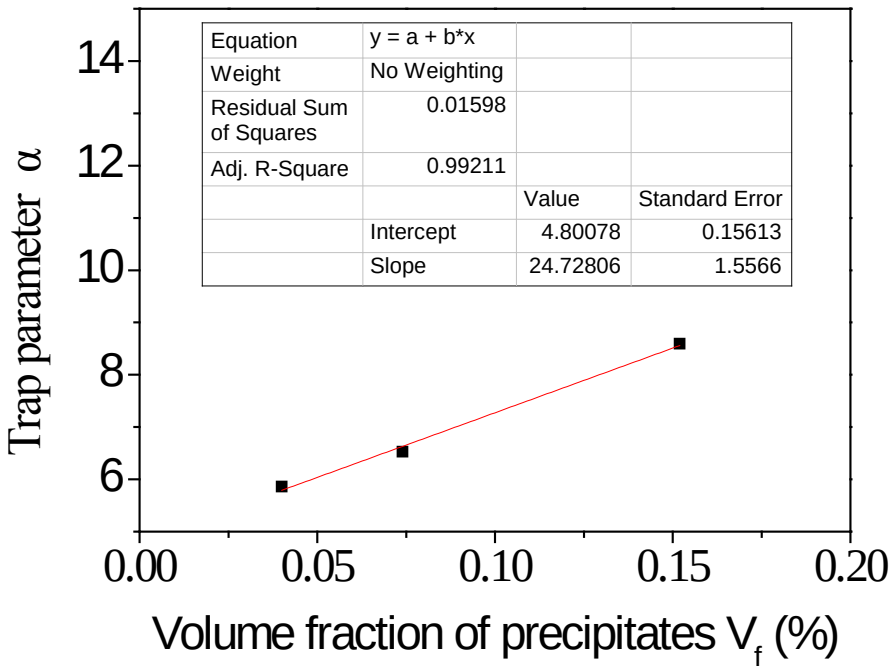

Fig. 5 Linear relationship between the trap parameter α and the volume fraction of precipitates V_f

Table 4 Hydrogen diffusion coefficients (at 293K) of the three steels

Sample	OTB	OCB	CB
D_{eff} calculated by Eq. (7)/($cm^2 \cdot s^{-1}$)	3.12×10^{-6}	3.91×10^{-6}	4.40×10^{-6}

2.4 Verification of model

Another low carbon heavy plate enameling steel, named TB, was also researched. The chemical composition of the TB steel is similar to the OTB steel. The hydrogen permeation experiments were repeated and the volume fraction of precipitates in TB steel was measured using the same method and parameter as the other three steels. The results are listed in Table 5. From Table 5, it can be seen that the D_{eff} calculated by the measured t_T and L is very close to the D_{eff} calculated by the developed model except the sample 3. The average value of the D_{eff} calculated by the model is higher than the average value of the D_{eff} calculated from the measured data at about 6%.

Table 5 Data of the TB steel at 293 K for verifying the model

	Sample 1	Sample 2	Sample 3	Average value
L/cm	0.0729	0.0735	0.0729	
t_T/s	250	248.5	293	
D_{eff} calculated by Eq. (3)/($cm^2 \cdot s^{-1}$)	3.54×10^{-6}	3.62×10^{-6}	3.02×10^{-6}	3.39×10^{-6}
V_f/%	0.099	0.094	0.113	0.102
D_{eff} calculated by Eq. (7)/($cm^2 \cdot s^{-1}$)	3.62×10^{-6}	3.67×10^{-6}	3.47×10^{-6}	3.59×10^{-6}

The room temperature model of correlation between D_{eff} and V_f for enameling steels was established successfully. It means the D_{eff} at room temperature can be calculated directly by the volume fraction of precipitates V_f (irreversible trapping sites) and vice versa. Actually there are other factors influencing the effective

hydrogen diffusion coefficient; even the volume fraction of precipitates is the same, the shape and distribution of the precipitates will also influence the hydrogen trapping effect. For this model, the precipitates were considered as round particles and the V_f is calculated by the Fullman equation based on the round particle shape.

2.5 Enameling experiment results

The both-side enameled heavy plates were checked by naked eyes, and no fishscales were found at the surfaces of enamel layers. But some traces of fishscales were found in the enamel layer of the CB steel samples sometimes, and no traces of fishscales were found in the OTB and OCB samples. The enamel layer and traces of fishscales are shown in Fig. 6. It was suggested that the hydrogen diffusion coefficient in porcelain enameling steels should be lower than 2.0×10^{-6} cm^2/s for preventing the occurrence of the fishscales[3], but the effective diffusion coefficients of the three steels developed are all higher than this criterion value when hydrogen permeation experiments were carried out at 20 ℃ (Table 3). The enameling experiment results show that no fishscaling happened on the OTB and OCB steels even the steels is both-side vitreous enameled. Then, the criterion value provided by Papp et al. [3] is not suitable for the developed hot rolled low carbon heavy plate steels for enameling.

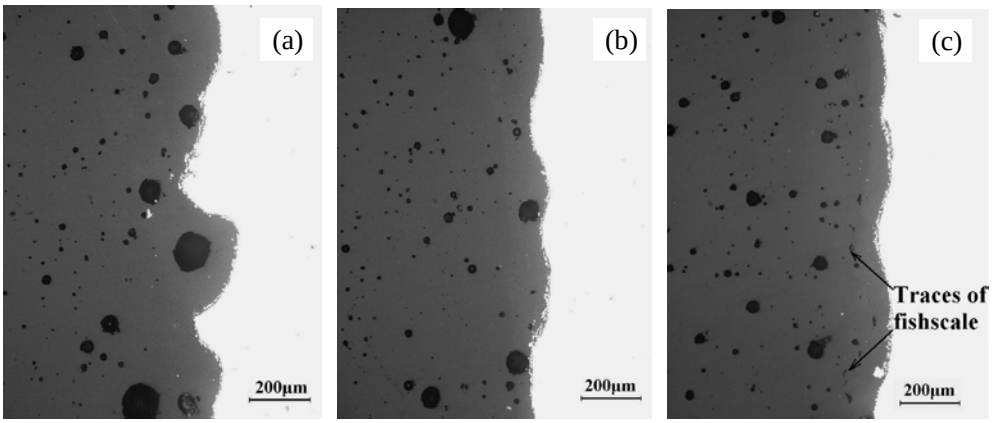

(a) OTB steel sample; (b) OCB steel sample; (c) CB steel sample.

Fig. 6 Vitreous enamel layer of three developed steels

According to the results of enameling experiment and the D_{eff} data listed in Table 3, the D_{eff} criterion value for judging the occurrence of fishscaling should be a number between 3.96×10^{-6} and 4.35×10^{-6} cm^2/s for hot rolled heavy plate steels, this means the effective hydrogen diffusion coefficient should be lower than 3.96×10^{-6} cm^2/s to avoid fishscaling for strictly speaking.

3 Conclusions

The TEM analysis results of precipitates show that the main particles in the OTB steel are coarse $Ti_4C_2S_2$ and fine Ti(C,N), main particles in the OCB and CB samples are fine Ti(C,N), and the volume fraction is in sequence of $V_{f(OTB)}>V_{f(OCB)}>V_{f(CB)}$. The hydrogen permeation experiments show that the effective hydrogen diffusion coefficient is in sequence of $D_{eff(OTB)}<D_{eff(OCB)}<D_{eff(CB)}$, which is in good agreement with the volume fraction of

precipitates in the steels. Precipitates can act as irreversible trapping sites for hydrogen and its volume fraction determines the effective hydrogen diffusion coefficient.

A room temperature model of correlation between the effective hydrogen diffusion coefficient and the volume fraction of irreversible trapping sites was established and verified. The D_{eff} at room temperature can be calculated directly by the volume fraction V_f of precipitates (irreversible trapping sites) and vice versa.

A new value for judging the fishscaling resistance of heavy plate steels was proposed. According to the experiment results and the model established, the effective hydrogen diffusion coefficient should be lower than 3.96×10^{-6} cm^2/s to avoid fishscaling in heavy plate steels. This value is nearly twice as the number reported by Papp et al. More accurate criterion value and the reason of the difference should be studied in future works.

References:

[1] K.H. Marshall, D. White, Vitreous Enamelling, Pergamon, Oxford, 1986.
[2] T. Okuyamas, A. Nishimoto, T. Kurokawa, Viterous Enameller, 41 (1990) No.3, 49-60.
[3] G. Papp, D. Geyer, G. Giedenbacher, Vitreous Enameller, 41 (1990) No.4, 71-81.
[4] H.H. Johnson, Hydrogen in iron, Metall. Trans. A, 19 (1988) No.10, 2371-2387.
[5] R.A. Oriani, Acta Metall. 18 (1970) No.1, 147-157.
[6] M.A.V. Devanathan, Z. Stachurki, Proc. R. Soc. Lond. A 270 (1962) No.1340, 90-102.
[7] R. Valentini, A. Solina, S. Matera, Metall. Trans. A 27 (1996) No.12, 3773-3780.
[8] T. Senuma, M. Kameda, M. Suehiro, ISIJ Int. 38 (1998) No.6, 587-594.
[9] M. Hua, C.I. Garcia, K. Eloot, A. J. DeArdo, ISIJ Int. 37 (1997) No.11, 1129-1132.
[10] N. Yoshinaga, K. Ushioda, S. Akamatsu, O. Akisue, ISIJ Int. 34 (1994) No.1, 24-32.
[11] I. Takahashi, Y. Matsumoto, I. Aruga, Kawasaki Steel Tech. Rep. 9 (1981) No.3, 57-64.
[12] Q.S. Sun, L. Jin, J. Iron and Steel Res. 19 (2007) No.4, 47-50.
[13] R. Valentini, A. Solina, L. Paganini, P. Degregorio, J. Mater. Sci. 27 (1992) No.1, 6579-6582.
[14] R. Valentini, A. Solina, L. Paganini, P. Degregorio, J. Mater. Sci. 27 (1992) No.1, 6583-6589.
[15] F. Fang, Q.L. Yong, C.F. Yang, Y.Q. Zhang, Acta Metallurgica Sinica 45 (2009) No.5, 625-629.
[16] W.Y. Choo, J.Y. Lee, Metall. Trans. A 14 (1983) No.7, 1299-1305.
[17] G.M. Pressouyre, I.M. Bernstein, Metall. Trans. A 9 (1978) No.11, 1571-1580.